(1+1) resonant enhanced multiphoton ionization via the A2Σ+ state of NO: Ionic rotational branching ratios and their intensity dependence

H. Rudolph, S. N. Dixit, V. McKoy, and W. M. Huo

Citation: J. Chem. Phys. **88**, 1516 (1988); doi: 10.1063/1.454130
View online: http://dx.doi.org/10.1063/1.454130
View Table of Contents: http://jcp.aip.org/resource/1/JCPSA6/v88/i3
Published by the American Institute of Physics.

(1+1) resonant enhanced multiphoton ionization via the $A\ ^2\Sigma^+$ state of NO: Ionic rotational branching ratios and their intensity dependence[a)]

H. Rudolph
Athur Amos Noyes Laboratory of Chemical Physics, California Institute of Technology, Pasadena, California 91125

S. N. Dixit
Lawrence Livermore National Laboratory, L-401, Livermore, California 94550

V. McKoy
Athur Amos Noyes Laboratory of Chemical Physics, California Institute of Technology, Pasadena, California 91125

W. M. Huo
NASA-Ames Research Center MS230-3, Moffett Field, California 94035

(Received 28 August 1987; accepted 20 October 1987)

Recent high resolution photoelectron spectroscopic studies of the (1 + 1) resonant enhanced multiphoton ionization (REMPI) of NO via the 0–0 transition of the A–X band (γ band) have shown a pronounced $\Delta N = 0$ signal ($\Delta N \equiv N_+ - N_i$) and smaller, but measurable, $\Delta N = \pm 2$ peaks. The authors [K. S. Viswanathan *et al.*, J. Phys. Chem. **90**, 5078 (1986)] assign the excitation to be via an $R(21.5)$ line, with no further specification. We have performed *ab initio* calculations of the rotational branching ratios for the four possible "$R(21.5)$" transitions, namely, the rotationally "clean" R_{21} and R_{22}, and the "mixed" $R_{12} + Q_{22}$ and $R_{11} + Q_{21}$ branches. We find the mixed $R_{12} + Q_{22}(21.5)$ branch to agree best with the observed photoelectron spectrum collected parallel to the polarization vector of the light. The discrepancy is larger for detection perpendicular to the polarization. To understand this difference, we have assessed the influence of laser intensity and polarization "contamination" on the branching ratios and photoelectron angular distributions.

INTRODUCTION

Within the past decade resonant enhanced multiphoton ionization spectroscopy (REMPI), combined with high resolution photoelectron spectroscopy (PES) has provided significant dynamical insight into several aspects of multiphoton ionization processes.[1–9] The REMPI-PES technique has been successfully employed in studies of diatomic molecules (H_2, NO, CO, N_2, I_2),[6–18] exploiting their less congested vibrational and rotational manifolds, which allows a greater specificity in the excitation schemes. The spectral resolution of the PES detectors have been refined to a point where the rotational structure of the ion can be resolved in the photoelectron spectra, providing information about the character of the resonant intermediate state, and on the electronic continuum.[6–8,14] Nitric oxide, NO, has attracted the most attention because of its low ionization potential (9.24 eV)[19] and its well-studied bound-bound spectrum.[20] Reilly and co-workers have, in a series of recent papers,[6–8] studied the lower Rydberg states of NO, with a photoelectron energy resolution (3 meV at best) sufficient to resolve the ionic rotational structure for medium to high rotational quantum numbers ($N \cong 10$–25). The agreement between the experimental and recently calculated[21–23] results has generally been quite good. Several important features in the PES were shown to arise from the nonspherical nature of the molecular potential. In a previous paper[21] we compared the calculated rotational branching ratios for (1 + 1) REMPI of NO via the $A\ ^2\Sigma^+$ ($3s\sigma$) state of NO to the earlier results of Wilson *et al.*[6] The agreement was moderately good and the observed photoelectron spectra could be explained on the basis of an "atomic-like" model, in which the $3s\sigma$ Rydberg state ejects a photoelectron primarily into the odd l partial waves of the electronic continuum. However, the analysis of the $D\ ^2\Sigma^+$ state PES indicates that the photoionization dynamics is more complex and that the "atomic" picture may be inadequate.

In this paper we present further detailed results on the (1 + 1) REMPI-PES via the $A\ ^2\Sigma^+$ state. As the rotational line in the data in Refs. 6 and 7 was identified as simply an $R(21.5)$ line, we present results for the four possible $R(21.5)$ transitions, two of which are "pure" and two are mixed rotational lines. The measured rotational branching ratios for parallel detection agree best with those calculated for the $R_{12} + Q_{22}(21.5)$ branch. The agreement in the perpendicular direction is less satisfactory. To assess the possible influence of saturation effects the solution of the rate equations for (1 + 1) REMPI is also analyzed.

THEORY

In this section we briefly describe the essential steps in the analysis of the (1 + 1) REMPI, and refer the reader to Refs. 24–26 for details. The (1 + 1) REMPI is viewed as a

[a)] Contribution no. 7650.

 0021-9606/88/031516-06$02.10

one-photon excitation to a resonant intermediate state (the $A\,^2\Sigma^+$ state) from an (initially) unaligned ground state (the $X\,^2\Pi$ state), followed by subsequent one-photon ionization out of this aligned intermediate state. The problem therefore has two parts: (i) a bound–bound excitation dynamical part and (ii) a bound–free photoionization part. We have in previous papers concerning NO concentrated our effort on the latter since the bound–bound dynamics can be adequately described by a simple perturbative scheme, where the population ρ_{ii} of the intermediate state's M_j sublevels are proportional to[24,26]

$$\rho_{ii} \propto \begin{pmatrix} J_0 & 1 & J_i \\ -M_i & 0 & M_i \end{pmatrix}^2 . \tag{1}$$

Here J_0 and J_i denote the total angular momentum quantum number for the $X\,^2\Pi$ and $A\,^2\Sigma^+$ states, respectively, and M_i the corresponding magnetic quantum number. This approximation is valid in the low laser intensity regime, where saturation and depletion effects can be neglected and in the absence of M_j mixing terms (linearly polarized light and collision free conditions, etc.). However, for moderately high laser intensities, Eq. (1) does not adequately describe the population of the intermediate state due to saturation effects. In this regime one has to use the density matrix equations. As explained previously by us[27] and others,[28–30] these reduce to a set of rate equations in the high intensity regime and under certain dephasing assumptions. The term high intensity regime is used rather loosely here, but generally refers to a situation where one or more of the excitation, fluorescence, or ionization rates are comparable to or larger than the reciprocal of the laser pulse duration (τ_p). In the saturation regime the REMPI process is quite sensitive to the laser characteristics and resonance conditions.

The ground $X\,^2\Pi$ state of NO belongs to the intermediate coupling case between Hund's cases (a) and (b), whereas the upper $A\,^2\Sigma^+$ state belongs strictly to Hund's case (b).[19,38] In the intermediate coupling regime, neither N, the nuclear rotational quantum number, nor Ω, the projection of the total angular momentum J on the internuclear axis ($\Omega = |\Lambda + \Sigma|$), is a good quantum number.[32,37,38] Each rotational level J is split into two components, f_1 and f_2, whose splitting depends on the spin–orbit coupling constant A and the rotational constant B. Λ doubling causes a further splitting of each of these components, but this is quite small for the $X\,^2\Pi$ state and will be neglected. The $A\,^2\Sigma^+$ state is in a similar fashion split into two sublevels (F_1 and F_2). This splitting is much smaller ($R = 8\times10^{-5}\,\mathrm{cm}^{-1}$)[20] than in the $X\,^2\Pi$ state and is unresolved in the current experiments. The various branches allowed by the one-photon dipole selection rule $\Delta J = 0, \pm 1$ are shown in Fig. 1. The notation for labeling the branches is ΔJ_{ij},[19] where i is the sublevel for the upper ($A\,^2\Sigma^+$) state and j for the lower ($X\,^2\Pi$) state. Whenever transitions to both J levels of a given N level in the A state are allowed one has a rotationally mixed branch. For a one-photon transition one therefore has rotationally clean P_{11}, R_{21}, P_{12}, and R_{22} branches, and rotationally mixed $Q_{11}+P_{21}$, $R_{11}+Q_{21}$, $Q_{12}+P_{22}$, and $R_{12}+Q_{22}$ branches as seen in Fig. 1. The photoionization dynamics therefore involves in the most general case a bound three level system: the initial

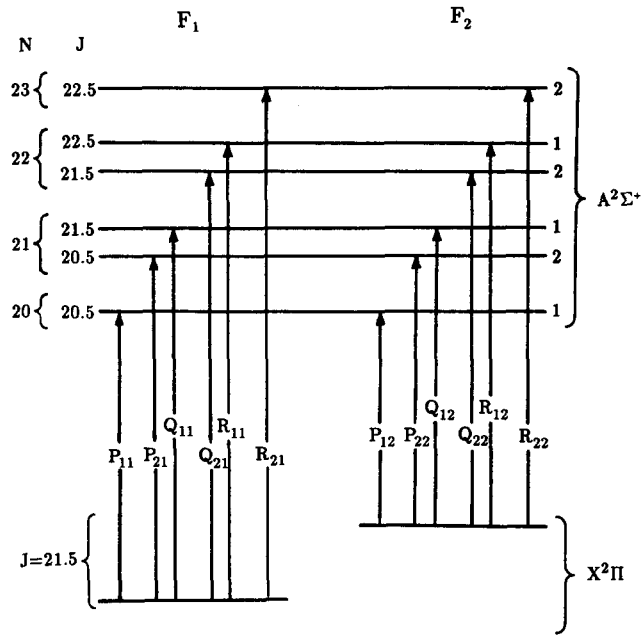

FIG. 1. The possible rotational branches originating from the $J = 21.5$ level of the $X\,^2\Pi$ state. The R_{1x} branches are mixed with the corresponding Q_{2x} ($X = 1$ or 2) branches because of the negligible splitting of the J-levels originating from the same N level of the upper state ($A\,^2\Sigma^+$ state).

state $|0\rangle$ and the two resonant intermediate states $|i\rangle$, and $|j\rangle$, which are coupled to the continuum $|k\rangle$ and described by the following rate equations[35]:

$$\frac{d\rho_{00}}{dt} = -W_{0i}(\rho_{00}-\rho_{ii}) - W_{0j}(\rho_{00}-\rho_{jj}), \tag{2a}$$

$$\frac{d\rho_{ii}}{dt} = W_{0i}(\rho_{00}-\rho_{ii}) - \sum_{N_+}\Gamma_i^{N_+}\rho_{ii}, \tag{2b}$$

$$\frac{d\rho_{jj}}{dt} = W_{0j}(\rho_{00}-\rho_{jj}) - \sum_{N_+}\Gamma_j^{N_+}\rho_{jj}, \tag{2c}$$

$$\frac{d\rho_{kk}^{N_+}}{dt} = (\Gamma_i^{N_+}\rho_{ii} + \Gamma_j^{N_+}\rho_{jj}). \tag{2d}$$

Here W_{0i} and W_{0j} are the excitation rates from the ground state to the two rotational sublevels

$$W_{0i} = K_{0i}S(J_0,J_i)\begin{pmatrix} J_0 & 1 & J_i \\ -M_i & 0 & M_i \end{pmatrix}^2 I(t), \tag{3a}$$

$$W_{0j} = K_{0j}S(J_0,J_j)\begin{pmatrix} J_0 & 1 & J_j \\ -M_j & 0 & M_j \end{pmatrix}^2 I(t), \tag{3b}$$

which are proportional to the laser intensity $I(t)$. The K_{0i} and K_{0j} factors depend on the ionization rates $\Gamma_i^{N_+}$ and $\Gamma_j^{N_+}$, as explained previously,[27] and on the laser bandwidth. In the following the K_{0i} and K_{0j} factors are assumed to be identical and their values taken from Ref. 31. $S(J_0,J_i)$ and $S(J_0,J_j)$ are the rotational line strengths as calculated originally by Earls.[32] The ionization widths $\Gamma_i^{N_+}$ and $\Gamma_j^{N_+}$ are defined as[27]

$$\Gamma_i^{N_+} = \frac{\sigma^{N_+}(M_i)I(t)}{h\nu}, \tag{4a}$$

$$\Gamma_j^{N_+} = \frac{\sigma^{N_+}(M_j) I(t)}{h\nu} . \tag{4b}$$

The rate equations (2) are valid in the low to the medium high intensity regime. The long lifetime of the A state ($\sim$200 ns) permits us to ignore the spontaneous emission rates γ_i and γ_j of the intermediate states (see Fig. 2). The two rotational sublevels of the intermediate states $|i\rangle$ and $|j\rangle$ are assumed to be incoherently excited. This assumption is justified because of strong dephasing due to laser bandwidth effects, shot-to-shot fluctuations, etc. For the excitation of a rotationally clean branch, Eqs. (2) reduce to a set of three rate equations that can be solved in closed form, but the four-level mixed-branch system must be solved numerically. Since different laser temporal profiles have previously been shown to have a minor effect (5%–10%) on the final results,[27,30] the shape of the laser pulse is assumed uniform. As seen by inspection, the rate equations of Eq. (2) do indeed yield the result of Eq. (1) in the low intensity regime.

The ionization cross section σ involves the sums of squares of the matrix element $r_{ki}^{l\lambda\mu}$,

$$r_{ki}^{l\lambda\mu} = \sum_{l',l_0} \langle \Psi_{kll'}(r) Y_{l'\lambda}(\hat{r}') | r Y_{1\mu}(\hat{r}') | \Phi_{il_0}(r) Y_{l_0 0}(\hat{r}') \rangle , \tag{5}$$

between the bound $|i\rangle$ and the final $|k\rangle$ state.[21] The electronic continuum wave function of the final state is calculated in the Hartree–Fock fixed-nuclei-frozen-core approximation using the variational Schwinger method[33] and includes the effects of the nonspherical, nonlocal nature of the molecular ion potential. The bound electronic wave function is calculated at the Hartree–Fock SCF level using a Gaussian basis set.[23]

Finally, the M_j-resolved photoelectron distribution $P_i^M(\theta)$ is given by

$$\frac{dP_i^M(\theta)}{dt} = \Gamma_i^M(\theta) \rho_{ii}^M(t) . \tag{6}$$

$P_i^M(\theta)$ can furthermore be expanded in terms of Legendre polynomials $P_L(\cos\theta)$:

$$P_i^M(\theta) = \sum_{L=0,2,\ldots} \beta_L^M(i) P_L(\cos\theta) . \tag{7}$$

In the high intensity limit, the upper limit on the summation is determined by the smaller of $2(J_i + 1)$ or $2 \cdot l_{\max}$, where $l_{\max}$ is the maximum partial wave retained in the expansion of the photoelectron continuum orbital. The resulting photoelectron angular distribution is the sum over all the M_j sublevels and branches (i) and integrated over the pulse duration τ_p,

$$P(\theta) = \sum_L P_L(\cos\theta) \sum_i \sum_{M_j} \beta_L^M(i) \int_0^{\tau_p} dt\, \rho_{ii}^M(t) . \tag{8}$$

Saturation effects in $P(\theta)$ in Eq. (8) appear through the intensity dependence of ρ_{ii}^M. The rotational branching ratios and the photoelectron angular distributions are obtained by the calculation of $P(\theta)$ for the different final rotational levels (N_+).

RESULTS

The recent experimental results by Viswanathan *et al.*[7] illustrate the branching ratios for (1 + 1) REMPI of NO via a $R(21.5)$ branch of the $A\,^2\Sigma^+$ state. As in their previous experiment[6] they observed only the even ΔN ($\Delta N \equiv N_+ - N_i$) terms, with the $\Delta N = 0$ signal as the dominating feature. The general selection rule for single photon ionization out of a Σ state leaving the ion in a Σ state,[25] is

$$\Delta N + l = \text{odd} , \tag{9}$$

where l is the partial wave of the photoelectron. Since the bound state is a $3s\sigma$ Rydberg state,[7,34] the $l = 1$ wave is predicted to be dominant in an atomic-like model, and hence ΔN is even. The previously reported calculated branching ratios were for the isolated (although in reality mixed) $R_{12}(21.5)$ or $R_{11}(21.5)$ branches. These branches lead to identical rotational branching ratios in the perturbative limit.[21] We have confirmed that the branching ratios are also essentially the same as those for the clean R_{22} and R_{21} branches, since the branching ratios change very little with N for such high values of J. The $\Delta N = 0$ signal indeed is the strongest, with a weak $\Delta N = \pm 1$ signal probably buried under the detection threshold. There are, however, as shown in Fig. 1, four possible $R(21.5)$ branches: the two clean R branches, R_{22} and R_{21}, and the two mixed branches, $R_{11} + Q_{21}$ and $R_{12} + Q_{22}$. The resonant wavelengths for these four branches are respectively, 2255.03, 2247.88, 2252.49, and 2259.67 Å.[19,20] The photoelectron kinetic energies for a $\Delta N = 0$ transition via (1 + 1) REMPI are all around 1.70 eV. As the actual wavelength used in the experiments of Refs. 6 and 7 was not quoted, the closeness of photoelectron kinetic energies makes it difficult to identify the specific $R(21.5)$ branch accessed in the experiment. Furthermore, there seems to be a slight difference between the $\Delta N = 0$ kinetic energy positions in the two published photoelectron spectra,[6,7] that may be caused by small changes in the surface potential in the electron spectrometer. In the following we will describe the calculation of the branching ratios via the four possible branches both in the perturbative limit and later in the high intensity limit.

The electronic wave function of the bound state is calcu-

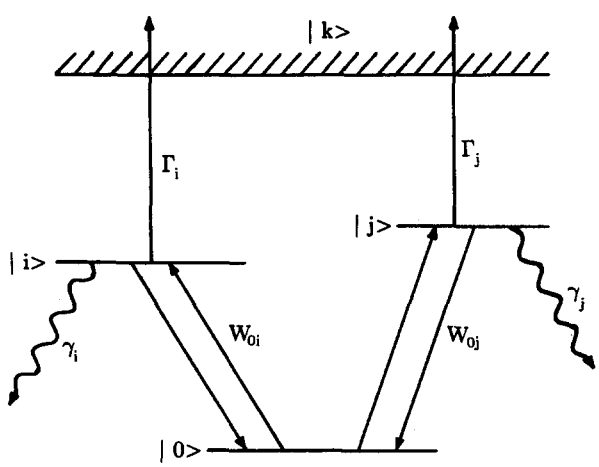

FIG. 2. Schematic picture of (1 + 1) REMPI via of the $A\,^2\Sigma^+$ state via a mixed rotational branch. The different constants are explained in the text.

lated with an extensive Gaussian basis set used in previous studies of higher members of the $^2\Sigma$ Rydberg series,[22,23] yielding a total electronic energy of -129.076 58 a.u. for a bond length of 1.062 Å, the equilibrium internuclear distance of the $A\,^2\Sigma^+$ state.[19] The single-center expansion of the 6σ orbital about the center of mass shows 94.0% s character, 0.3% p character, 5.4% d character, 0.1% f character, and 0.2% g character in agreement with our previous results[21] and the results of Kaufmann *et al.*[34] For a kinetic energy of 1.67 eV, corresponding to the $\Delta N = 0$ signal of the observed $R(21.5)$ band, the relative magnitudes of the $|r_{ki}^{\mu_i\mu}|^2$ of Eq. (5) are 0.038, 0.091, 0.048, 0.119, and 0.005 for $l = 0,4$ in the $k\sigma$ channel, and 0.299, 0.014, 0.173, and 0.007 for $l = 1,4$ in the $k\pi$ channel. As expected the ionization out of the primarily gerade (even l) bound 6σ orbital gives rise to a primarily ungerade character of the continuum, and it is seen that the π channel contributes the major part (0.804 Mb) of the total cross section (1.158 Mb). These cross sections are in agreement with our previous results,[21] and the experimental results of Rottke and Zacharias.[28]

In Fig. 3, we compare the experimental and the calculated branching ratios for parallel and perpendicular (relative to the polarization of the radiation) detection for the three different branches. The $R_{22}(J)$ and $R_{21}(J)$ branches have identical normalized branching ratios in the perturbative limit, since the only difference is the rotational line strength $S(J_0, J_i)$, which for clean branches is an overall factor. The rotational line strengths are[32] $R_{11}(21.5) = 4.212$, $R_{12}(21.5) = 1.166$, $R_{21}(21.5) = 1.373$, $R_{22}(21.5) = 4.005$, $Q_{21}(21.5) = 2.596$, and $Q_{22}(21.5) = 8.398$. The mixed $R_{12} + Q_{22}$ and $R_{11} + Q_{21}$ branches have been weighted appropriately with these factors, and the resulting branching ratios convoluted with a Lorentzian detection function with a FWHM of 6 meV. They are shown on the same absolute energy scale as the experimental results.[6,7] The normalized branching ratios for both directions of detection (normalized to the $\Delta N = 0$ signal in each branch) are given in Table I. The calculated relative intensities for the $\Delta N = 0$ signals for the four branches are $R_{12} + Q_{22} = 1.000$, $R_{11} + Q_{21} = 0.5006$, $R_{22} = 0.1989$, and $R_{21} = 0.0682$. Comparison to the experimental results suggests that the most likely candidate among these branches is the mixed $R_{12} + Q_{22}(21.5)$ branch. It is also seen, that the $\Delta N = \pm 1$ signals, although present, are embedded in the strong $\Delta N = 0$ signal, and therefore not experimentally observable.

TABLE I. Rotational branching ratios for the laser light polarized parallel ($\theta = 0°$) and perpendicular ($\theta = 90°$) to the detection direction (perturbative limit). The branching ratios are normalized to the $\Delta N = 0$ signal.

Parallel detection ($\theta = 0°$)				
ΔN	$R_{22}(21.5)$	$R_{21}(21.5)$	$R_{11} + Q_{21}(21.5)$	$R_{12} + Q_{22}(21.5)$
−2	0.292	0.292	0.142	0.050
−1	0.041	0.041	0.020	0.007
0	1.000	1.000	1.000	1.000
+1	0.042	0.042	0.021	0.008
+2	0.301	0.301	0.156	0.061
Perpendicular detection ($\theta = 90°$)				
ΔN	$R_{22}(21.5)$	$R_{21}(21.5)$	$R_{11} + Q_{21}(21.5)$	$R_{12} + Q_{22}(21.5)$
−2	1.916	1.916	1.388	0.881
−1	0.125	0.125	0.123	0.120
0	1.000	1.000	1.000	1.000
+1	0.125	0.125	0.129	0.132
+2	2.025	2.025	1.520	0.998

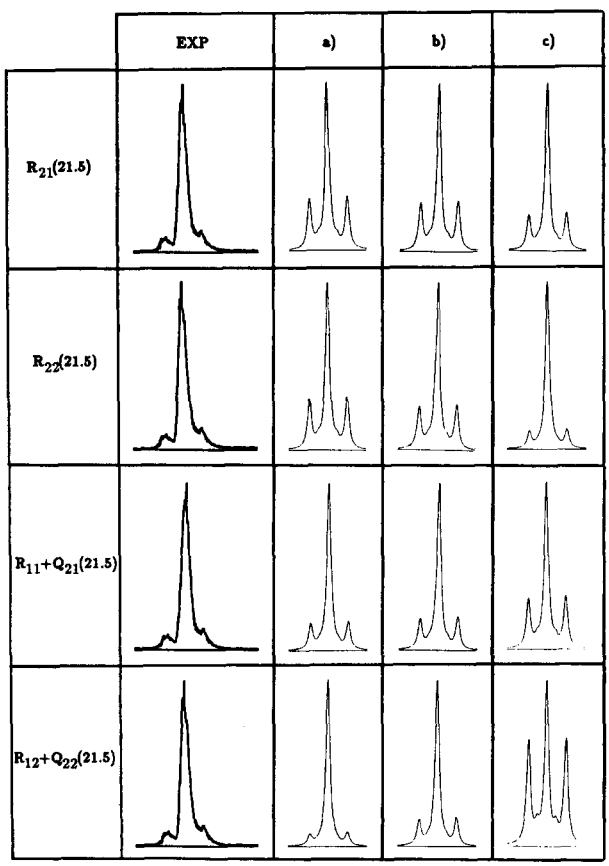

FIG. 3. Comparison of the experimental (left) and the calculated (right) rotational branching ratios for the three possible branches: (a) R_{21} or R_{22}; (b) $R_{11} + Q_{21}$; and (c) $R_{12} + Q_{22}$ for the light polarization parallel ($\theta = 0°$) and perpendicular ($\theta = 90°$) to the direction of detection (perturbative limit).

Agreement between the experimental and the calculated branching ratios is less satisfactory for perpendicular detection than for parallel detection. The experimentally observed strong $\Delta N = 0$ signal is only partly reproduced in the calculated branching ratios, with the best agreement once again for the mixed $R_{12} + Q_{22}(21.5)$ branch. This discrepancy could in part be caused by the finite width of the detector in combination with the forward peaked (around $\theta = 0°$) angular distribution for the $\Delta N = 0$ peak. (See Fig. 6). Averaging the signal over a finite detector acceptance angle for a realistic width of 3° did not improve the agreement. The perpendicular signal is calculated to be about 50 times weaker than the parallel signal. Even a small experimental misalignment or less than 100% linearly polarized light could lead to a "contamination" of the perpendicular signal by the parallel signal. With this large difference in the signal

of the perpendicular signal by the parallel signal is sufficient to cause the measured "perpendicular" signal to have a substantially stronger $\Delta N = 0$ peak, as experimentally observed.[7] We will, however, in the following assume the system to be aligned and the light source to be 100% linearly polarized. Another possible reason for this discrepancy between theory and experiment could be high intensity effects, arising from the higher laser intensity necessary to achieve a detectable signal in the perpendicular case.

To estimate the effects of saturation, we have calculated relative branching ratios at various laser intensities by directly solving the rate equations (2). The K_{0i} and K_{0j} are assumed equal, and their values are taken from Ref. 31. The rate equations are integrated nummerically under the assumption of a constant laser bandwidth and detection function (FWHM = 6 meV). The resulting branching ratios, as a function of intensity, are shown in Fig. 4 for parallel detection and in Fig. 5 for the perpendicular detection. It is seen that the branching ratios for the R_{22} and the R_{21} branches, which were identical in the perturbative limit, do change with higher laser intensities, and that the $\Delta N = 0$ peak for the mixed branches becomes less dominant at higher intensities. The perpendicular signal shows the same trend which is opposite to that seen experimentally. The differences are hence probably due to effects not incorporated in the present study.

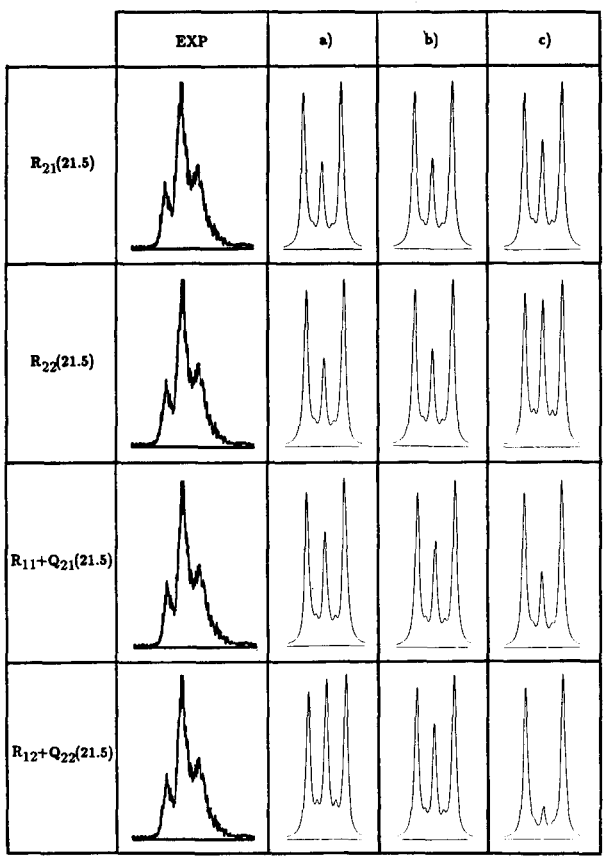

FIG. 4. Comparison of the experimental (left) and the calculated (right) branching ratios as a function of laser intensity, for detection along the direction of polarization. The total energy per unit area is (a) 1.0 J cm^{-2}, (b) 10 J cm^{-2}, and (c) 50 J cm^{-2}.

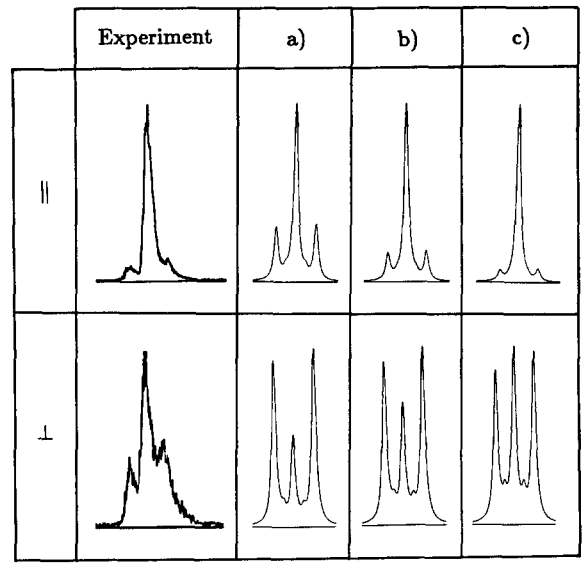

FIG. 5. Same as Fig. 4, but for detection perpendicular to the light polarization direction.

For higher laser intensities saturation effects will give rise to higher β values (higher than the perturbative limit of β_4).[24] The magnitude of the higher β values depend on the relative saturation rates for the different M_j channels. The photoionization cross sections are nearly constant for the different M_j sublevels, as found experimentally by Jacobs *et al.*[31] and theoretically by us.[21] Therefore, the terms beyond β_4 will have finite values for higher field intensities although their magnitudes are expected to be small. In fact, our calculations indicate that the only higher β value of significance is the β_6 value, and it never becomes larger than 5% of the β_0 value. The photoelectron angular distributions for the different rotational branches ($\Delta N = 0, \pm 1, \pm 2$) ionized via the $R_{12} + Q_{22}(21.5)$ branch are plotted in Fig. 6 as a function of intensity. It is seen that the photoelectron angular distribution for the $\Delta N = 0$ signal in the perturbative (low intensity) limit are strongly peaked around $\theta = 0°$ and that the distributions for the different ΔN signals become similar for higher intensities.

CONCLUSIONS

We have discussed rotational branching ratios resulting from the (1 + 1) REMPI of NO via the 0–0 transition of the A–X band (γ band) for the four possible branches that can be assigned as $R(21.5)$. The calculations were done in the frozen-core approximation at the Hartree–Fock level. The four different branches, of which three are distinctly different in the perturbative limit, have rather different branching ratios. The mixed $R_{12} + Q_{22}(21.5)$ branch, which is most intense and has the lowest transition energy, seems to give the best agreement with the experimental branching ratios for parallel detection. For perpendicular detection the agreement is less satisfactory. Neither the effect of finite-acceptance angle of the photoelectron detector nor high intensities can explain the discrepancy.

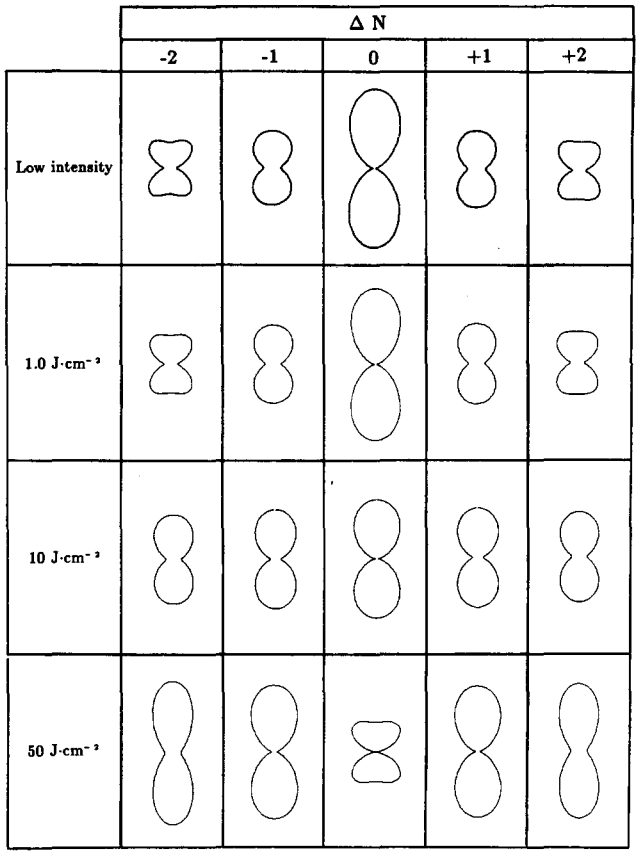

FIG. 6. Photoelectron angular distributions as a function of total laser intensity for the different rotational lines. $\beta_0 \equiv 1.00$ for all the rotational lines.

ACKNOWLEDGMENTS

This material is based on research supported by the National Science Foundation under Grant No. CHE-8521391, by AFOSR under Grant No. 87-0039, by the office of Health and Environmental Research of DOE (DE-FG03-87ER60513), and by NASA Cooperative Agreement NCC2-319. Work done by S. N. D. was performed under the auspices of the U. S. Department of Energy by Lawrence Livermore National Laboratory under Contract No. W-7405-Eng-48. H. R. gratefully acknowledges the support of the Danish Natural Science Research Council.

[1]J. P. Booth, S. L. Bragg, and G. Hancock, Chem. Phys. Lett. **113**, 509 (1985).
[2]P. Chen, J. B. Ballix, W. A. Chupka, and S. D. Colson, J. Chem. Phys. **86**, 516 (1987).
[3]R. G. Evans and P. C. Thonemann, Phys. Lett. A **38**, 398 (1972).
[4]Y. Nagano, Y. Achiba, and K. Kimura, J. Chem. Phys. **84**, 1063 (1986).
[5]Y. Achiba, K. Sato, K. Shobatake, and K. Kimura, J. Chem. Phys. **79**, 5213 (1983).
[6]W. G. Wilson, K. S. Viswanathan, E. Sekreta, and J. P. Reilly, J. Phys. Chem. **88**, 672 (1984).
[7]K. S. Viswanathan, E. Sekreta, E. R. Davidson, and J. P. Reilly, J. Phys. Chem. **90**, 5078 (1986).
[8]K. S. Viswanathan, E. Sekreta, and J. P. Reilly, J. Phys. Chem. **90**, 5658 (1986).
[9]M. G. White, M. Seaver, W. A. Chupka, and S. D. Colson, Phys. Rev. Lett. **49**, 28 (1982).
[10]S. T. Pratt, P. M. Dehmer, and J. L. Dehmer, J. Chem. Phys. **78**, 4315 (1983).
[11]S. T. Pratt, P. M. Dehmer, and J. L. Dehmer, Chem. Phys. Lett. **105**, 28 (1984).
[12]S. L. Anderson, G. D. Kubiak, and R. N. Zare, Chem. Phys. Lett. **105**, 22 (1984).
[13]J. C. Miller and R. N. Compton, J. Chem. Phys. **84**, 675 (1986).
[14]K. Müller-Dethlefs, M. Sander, and W. Schlag, Chem. Phys. Lett. **112**, 291 (1984).
[15]S. T. Pratt, E. D. Poliakoff, P. M. Dehmer, and J. L. Dehmer, Chem. Phys. **78**, 65 (1983).
[16]S. T. Pratt, P. M. Dehmer, and J. L. Dehmer, J. Chem. Phys. **79**, 3234 (1983).
[17]S. T. Pratt, P. M. Dehmer, and J. L. Dehmer, J. Chem. Phys. **81**, 3444 (1984).
[18]J. C. Miller and R. N. Compton, J. Chem. Phys. **75**, 2020 (1981).
[19]K. P. Huber and G. Herzberg, *Constants of Diatomic Molecules* (Van Nostrand Reinhold, New York, 1979).
[20]R. Engleman, Jr., P. E. Rouse, H. M. Peek, and V. D. Baiamonte, Los Alamos Report, LA-4364, UC-34 Physics, TID-4500 (Los Alamos, Laboratory Los Alamos, 1970).
[21]S. N. Dixit, D. L. Lynch, V. McKoy, and W. M. Huo, Phys. Rev. A **32**, 1267 (1984).
[22]H. Rudolph, S. N. Dixit, V. McKoy, and W. M. Huo, Chem. Phys. Lett. **137**, 521 (1987).
[23]H. Rudolph, S. N. Dixit, V. McKoy, and W. M. Huo, J. Chem Phys. **88**, 1516 (1988).
[24]S. N. Dixit and V. McKoy, J. Chem. Phys. **82**, 3546 (1985).
[25]S. N. Dixit and V. McKoy, Chem. Phys. Lett. **128**, 49 (1986).
[26]S. N. Dixit, D. L. Lynch, and V. McKoy, Phys. Rev. A **30**, 3332 (1984).
[27]H. Rudolph, D. L. Lynch, S. N. Dixit, and V. McKoy, J. Chem. Phys. **84**, 6657 (1986).
[28]H. Rottke and H. Zacharias, J. Chem. Phys. **83**, 4831 (1985).
[29]V. S. Letokhov, V. I. Mishin, and A. A. Puretzky, *Prog. Quantum Electr.* (Pergamon, London, 1977), Vol. 5, p. 139.
[30]D. C. Jacobs and R. N. Zare, J. Chem. Phys. **85**, 5457 (1986).
[31]D. C. Jacobs, R. J. Madix, and R. N. Zare, J. Chem. Phys. **85**, 5469 (1986).
[32]L. T. Earls, Phys. Rev. **48**, 423 (1935).
[33]R. R. Lucchese, G. Raseev, and V. McKoy, Phys. Rev. A **25**, 2572 (1982).
[34]K. Kaufmann, C. Nager, and M. Jungen, Chem. Phys. **95**, 385 (1985).
[35]S. N. Dixit and P. Lambropoulos, Phys. Rev. A **27**, 861 (1983).
[36]C. H. Green and R. N. Zare, J. Chem. Phys. **78**, 674 (1983).
[37]G. Herzberg, *Spectra of Diatomic Molecules* (Van Nostrand Reinhold, New York, 1950).
[38]B. R. Judd, *Angular Momentum Theory for Diatomic Molecules* (Academic, New York, 1975).